Establishment of an Animal Model of Oral Squamous Cell Carcinoma Invading the Mandible

Xiang Long ZHENG[1], Kang Wei ZHOU[1], Wen LI[1], Ya Qi CHEN[1], Cheng Hui LU[2], Li Song LIN[1]

Objective: *To establish an animal model of oral squamous cell carcinoma invading the mandible through multi-sample experiments that verified the stability, repeatability, tumorigenicity and mandible destruction rate of the model.*

Methods: *Oral squamous cell carcinoma cell suspension was injected into the outer side of the mandible through the anterior edge of the masseter muscle of naked mice to observe the tumour-forming process. Then, the anatomical, histological and imaging examinations were carried out to determine whether the tumour had invaded the mandible. By comparing the tumour growth of multiple groups of various squamous cell carcinoma cells (CAL27, HN6 and HN30 cells), the changes in body weight and characteristics of tumour formation were compared, and the experience was summarised to further verify the stability, repeatability, tumour formation rate and arch damage rate of the model.*

Results: *The subsequent specimens of tumour-bearing nude mice were validated once the model had been established. In vitro, tumour tissue wrapped around the mandible's tumour-bearing side, and the local texture was tough with no resistance to acupuncture. Haematoxylin and eosin staining revealed that squamous cells were infiltrating the mandible in both the horizontal and sagittal planes. Microcomputed tomography results showed that the mandible on the tumour-bearing side displayed obvious erosion damage. Cell lines with various passage rates clearly had diverse tumour-bearing life cycles.*

Conclusion: *This study successfully established an animal model of oral squamous cell carcinoma invasion of the mandible. The model has excellent biological stability, repeatability, tumorigenesis rate and mandible destruction rate.*

Keywords: *animal model, invade, life cycle, mandible, oral squamous cell carcinoma*
Chin J Dent Res 2024;27(3):235–241; doi: 10.3290/j.cjdr.b5698375

Oral squamous cell carcinoma (OSCC) is one of the most common malignant tumours in the head and neck, and surgery is still the main treatment method.[1,2] With the development of existing diagnosis and treatment technology, although the survival rate with early-stage OSCC can reach up to 80%, the 5-year survival rate of middle- and late-stage patients is still approximately 50%.[3,4] The main causes include local recurrence, lymph node metastasis and distant metastasis.[5] Even if the tumour is completely removed with an appropriate margin of safety during surgery, local recurrence may still occur. Especially when the tumour invades the jawbone, due to high bone density and hard cortical bone, rapid frozen section and other methods cannot be used to detect the operative bone incisal margin without decalcification. In addition, the interface of OSCC infiltrating the jawbone cannot be accurately defined through imaging examination before surgery,[6,7] so it is difficult to con-

1 Department of Oral and Maxillofacial Surgery, The First Affiliated Hospital, Fujian Medical University, Fuzhou, P.R. China.
2 School and Hospital of Stomatology, Fujian Medical University, Fuzhou, P.R. China.

Corresponding author: Dr Li Song LIN, Department of Oral and Maxillofacial Surgery, The First Affiliated Hospital, Fujian Medical University, No.20 Cha-Zhong Road, Fuzhou 350005, Fujian Province, P.R. China. Tel: 86-13905006502 Email: dr_lls@hotmail.com

This work was supported by Joint Funds for the Innovation of Science and Technology of Fujian province (no. 2019Y9128)

firm whether the bone incisal margin is negative during the procedure. Thus, it is impossible to resect the diseased jaw tissue safely and accurately.[8]

The types of bone invasion include erosion, infiltration and mixed patterns,[9] but the specific mechanism and mode of invasion have not been defined. Various animal models have developed to study the pathogenesis, genetic background and novel therapeutic development of OSCC.[10] The information obtained from animal models is crucial for the diagnosis and treatment of OSCC; however, no single model can summarise all aspects, and the corresponding animal models need to be constructed for different studies.[11] To further study the specific mechanism or means of invasion of the mandible by OSCC, it is necessary to establish a corresponding animal model to better reflect the invasion of mandible by human tumours.

Despite the fact that there are several animal models for oral cancer, only a very small portion of research has so far focused on the animal model of OSCC invading the mandible,[12-14] and none of these studies have gone into great depth on the modelling approach, tumorigenicity rate or success rate. The objective of the present study was to investigate and summarise the animal models of OSCC invading the mandible. It also aimed to establish a stable and repeatable animal model of OSCC invading the mandible with high tumorigenicity by implementing repeated experiments on multiple samples with comprehensive verification of anatomy, pathology and imaging.

Materials and methods

Reagents and instruments

Dulbecco's modified Eagle's medium (DMEM), 10% foetal bovine serum (FBS) and 0.25% trypsin (Gibco, Billings, MT, USA) were employed, along with a CBCT machine for dentistry (Kawa Group, Biberach, Germany); microcomputed tomography (microCT) machine (SCANCO Medical, Brüttisellen, Switzerland), 4% paraformaldehyde fixative (Guangzhou Saiguo Biotechnology, Guangzhou, China), isothane (Reward Life Sciences, Shenzhen, China and SCANCO Medical), isoflurane (Reward Life Sciences), ethylenediaminetetraacetic acid (EDTA) decalcification solution (Solarbio, Beijing, China), neutral gum (Taipu Biological, Xiamen, China) and haematoxylin-eosin (HE) staining solution (Xiamen Taipu Biological).

Cell culture

Human-derived OSCC cell lines CAL27 cells, HN6 cells, HN30 cells (Shanghai Zhongqiao Xinzhou Biological Company, Shanghai, China) were cultured in DMEM high glucose medium containing 10% FBS in a humidified incubator with an atmosphere containing 5% CO_2 at 37°C, and trypsin digestion was used for passaging when the cells were fused to 80%.

Animal feeding and grouping

Fifteen male BALB/c nude mice aged 3 to 5 weeks old, with a body mass of around 15 g, were purchased from Shanghai Slaughter Laboratory Animal Co, Ltd, China. All of the animal procedures were conducted in accordance with the Guidelines for the Care and Use of Laboratory Animals and were approved by the Institutional Animal Care and Use Committee at Fujian Medical University. Nude mice were acclimatised to the specific pathogen free (SPF) environment for 1 week, and the experiments were started at a body weight of around 20 g. The feeding environment was set at room temperature of 20°C to 22°C, humidity of 40% to 70%, and a light/dark cycle of 12 hours. The mice were supplied with adequate drinking water and feed.

The fifteen nude mice were randomly divided into three groups of five mice each, namely the CAL27 cell group, HN6 cell group and HN30 cell group. After the tumour was planted, the weight of the nude mice was recorded every other day, and the nude mice were sacrificed when the tumour size reached 1 cm^3 or the weight decreased by 25% of the original weight, and the mandibular bone and tumour tissues were taken from the tumour-bearing side.

Tumour cell suspension preparation

When the cell confluence reached around 80% to 90% of the whole bottom of the dish, trypsin digestion was complete, and complete medium was added to terminate the digestion, blowing the cells at the bottom of the dish until all the cells at the bottom of the dish were dislodged; the liquid in the dish was transferred into a centrifuge tube, centrifuged (4°C, 1000 rpm, 5 minutes), and then the supernatant was discarded; 2 ml iced PBS was added to fully resuspend the cells, and 20 µl of the liquid was taken into the cell counting plate, and the cells in the same grid were counted in three different fields of view, and the mean was calculated. The total number of cells contained in 2 ml PBS was calculated by centrifugation and the supernatant was discarded, and

the total number of cells was adjusted to a cell density of 1×10^6 cells/0.1 ml by adding an appropriate amount of iced PBS, and then the cell suspensions were transferred into 2 ml Eppendorf (EP) tubes.

Establishment of animal model

After the nude mice were administered anaesthesia by a small animal gas anaesthesia machine, the appropriate concentration of anaesthetics was continuously administered for maintenance; the cell suspension was prepared and was gently blown out with a pipette gun before the cells were aspirated by a syringe, and the insulin injection needle was used to aspirate 0.1 ml of cells; the nude mice were disinfected with iodine violet in the right masseter area, and then the needle was inserted inwards and backwards at the horizontal level of the lower edge of the biting muscle, with the angle of needle insertion (Fig 1a) being parallel to the bone surface of the mandible, and the needle insertion was roughly 6 mm in length. When the tip of the needle was felt on the outer face of the mandible, the cell suspension was injected slowly, and the injection was observed while injecting. The injection was successful if there was localised elevation and no liquid oozing out of the mouth, and the injection needle was quickly withdrawn after the injection was completed to avoid leakage of the cell solution. The nude mice were put back into their cages to be reared after recovering their mobility.

HE staining

Different levels (sagittal and horizontal) of mandibular tissues were taken for HE staining, and the fixed mandibles were paraffin-embedded, prepared into 4-μm-thick sections from the horizontal and sagittal planes of the mandible, stained with HE, sealed with neutral gum and observed under a microscope.

MicroCT assay

The specimen was removed from the fixative and wrapped in three to four layers with plastic wrap to retain moisture. It was placed in a sample tube with a diameter of 34 mm, stuffed with cotton to fix it to avoid artifacts caused by movement of the specimen during the scanning process and fixed so that the sample rested on the bottom of the tube, and then placed in the scanning instrument (SCANCO Medical, μCT100) for scanning.

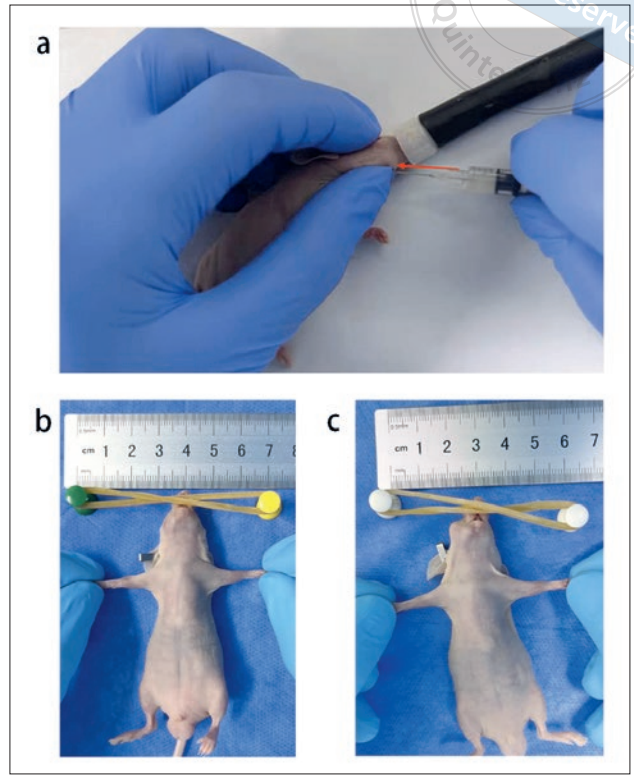

Fig 1a to c Moulding process. The red arrow indicates the needle entry angle **(a)**. The early stage of tumor bearing **(b)**. Later stage of tumour bearing **(c)**.

Statistical analysis

SPSS 25.0 software (IBM, Chicago, IL, USA) was used for statistical analysis. The level of statistical significance was set at $P < 0.05$. One-way ANOVA showed that there was no significant difference in the body weight of nude mice at the time of tumour implantation between the groups ($P > 0.05$), but there was a significant difference in the survival cycle between the groups after tumour implantation ($P < 0.05$).

Results

Anatomical specimen verification

The cranial specimen of nude mice that met the standards for execution (Fig 2a) showed that the lateral occlusal muscle of the jaw on the normal side was not covered by tumour tissue. The normal side of the jaw was entirely peelable and hard when the right and left mandibles were separated, and tumour tissue had attached to the ascending branch of the mandible (Fig 2b). The posterior edge of the jaw was firm and offered little re-

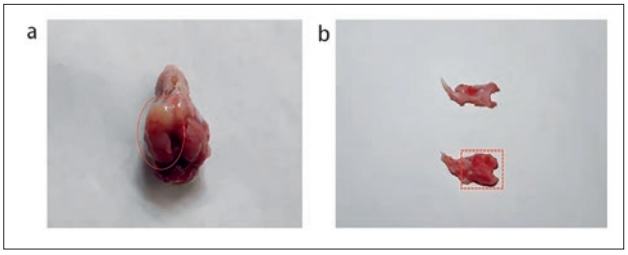

Fig 2a and b Anatomical specimens. Skull specimen; the red dotted area is the lateral mandibular tumour on the tumour-bearing side **(a)**. Mandible specimen; the upper part of the figure is the normal side of the mandible, the mandible anatomical shape is complete and hard; the lower part is the tumour-bearing mandible. The red dotted line shows that the posterior margin of the mandible is wrapped with tumor tissue and is locally tough **(b)**.

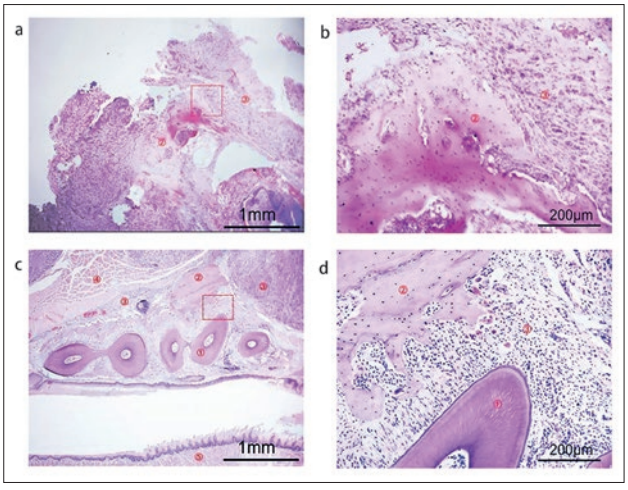

Fig 3a to d HE staining at different levels. Sagittal position of the mandible on the tumour-bearing side (40×); dotted line frame is shown by b **(a)**. Sagittal position of the mandible on the tumour-bearing side (200×) **(b)**. The area shown in **(a)** and **(b)** is a certain level of the ascending branches of the mandible from the side view, which show that the ascending branches of the mandible are eroded by tumour tissue. Horizontal position of the mandible on the tumour-bearing side (40×), as shown by dashed line box d **(c)**. The horizontal position of the mandible on the tumour-bearing side (200×) **(d)**. The areas shown in **(c)** and **(d)** are a certain level of the posterior teeth and buccal side of the mandible horizontal plane, and the masseter muscle, mandible and around the root of the tooth are all invaded by tumour cells. (Note: 1, teeth; 2, mandible; 3, tumour cells; 4, muscle; 5, tongue.)

sistance to needling, and the tumour profile was milky white.

Pathological verification

The isolated mandibular tissue underwent various levels of histological staining (Fig 3). Section staining from the lateral side of the mandible revealed that squamous carcinoma cells had infiltrated and extensively destroyed the bone of the ascending mandibular branch at a specific level (Fig 3a and b), whereas section staining from the horizontal plane showed that the homogeneous side of the mandible at the same level had also been extensively destroyed by tumour cells (Fig 3c and d).

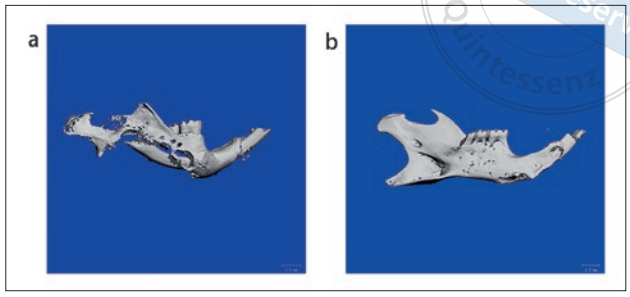

Fig 4a and b MicroCT of the mandible. The tumour-bearing side of the mandible showed that the mandibular bone was clearly damaged **(a)**. Normal lateral mandible; the visible mandible anatomical structure is complete **(b)**.

Imaging verification

Although the success of the model establishment was essentially verified through a combination of anatomical specimens and histological validation, microCT was performed as a supplement to the anatomical and pathological results to obtain additional 3D validation, as shown in Fig 4. This image demonstrates that, in comparison to the normal side of the mandible, the loaded side of the tumour clearly caused damage to the mandibular bone, and localised erosive destruction was visible.

Clinical manifestations of different oral squamous carcinoma cells invading the mandible

The HN30 and HN6 groups showed faster tumour formation, within just 1 week, whereas the CAL27 group had a noticeably slower tumour formation rate during the growth of the nude mice. The tumour-side samples of three different groups of oral squamous carcinoma cells invading the mandible were photographed and compared after the nude mice were sacrificed (Fig 5). The tumour cycles of the HN30 group were only about 18 days after tumour growth (Fig 5a, c and e), those for the HN6 group were 26 days, and those for the CAL27 group could be up to 52 days (Fig 5b, d and f), but there was no statistically significant difference in the changes in body weight between the groups.

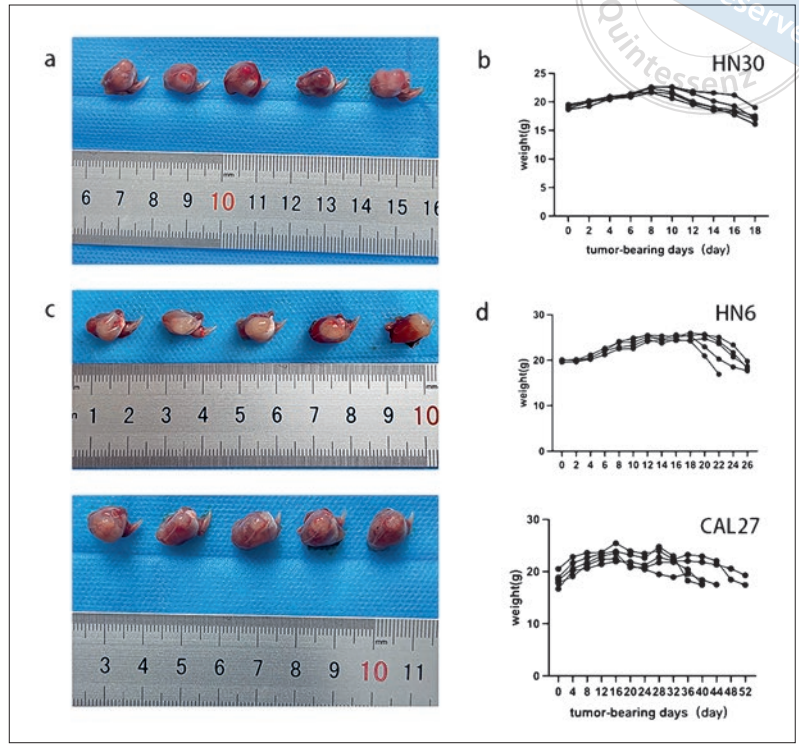

Fig 5a to f Curve of body weight and specimen after tumour formation. The mandibular specimens of the HN30 **(a)**, HN6 **(c)** and CAL27 groups **(e)** were obtained after meeting the execution criteria. Body weight change curves of the HN30 **(b)**, HN6 **(d)** and CAL27 groups **(f)** during tumour-bearing, respectively.

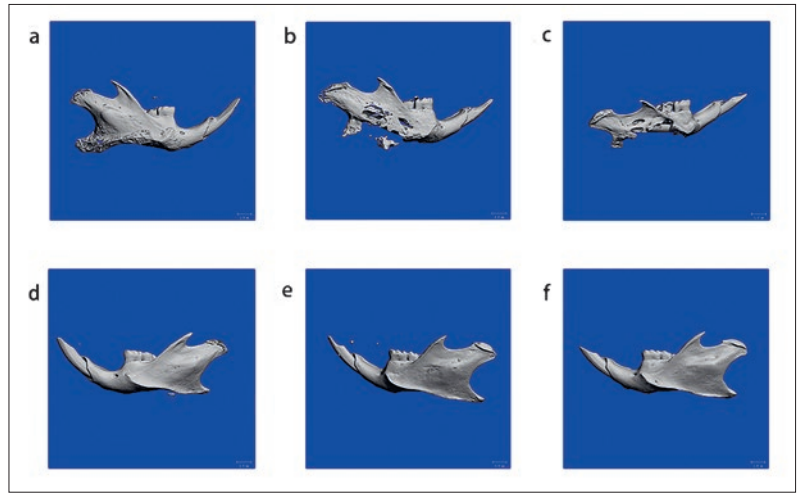

Fig 6 MicroCT of the mandible. The tumour-bearing mandibles in the HN30 **(a)**, HN6 **(b)** and CAL27 groups **(c)** showed different degrees of bone destruction of the mandible. Normal lateral mandibles in the HN30 **(d)**, HN6 **(e)** and CAL27 group **(f)**, indicating complete mandibular anatomy.

Imaging manifestations of mandibular invasion by different OSCC cells

MicroCT examination of three groups of nude mice was performed, and it was found that the HN6 and HN30 group did not cause more obvious destruction to the mandible due to the rapid growth of the tumour. The results of microCT examination between the different groups revealed that, regardless of which OSCC cells were injected at the same injection concentration, the longer the survival cycle of nude mice with tumours, the more extensive the destruction of the mandible; in contrast, the shorter the survival time of the tumour, the smaller the degree of destruction of the mandible (Fig 6).

Discussion

From 1954, when Salley[15] coated the buccal sac of the golden gopher with dimethylbenzanthracene (DMBA) to make it malignant, to the present, when numerous animal models of oral cancer are frequently utilised,

diverse modelling techniques have been available for various studies. Reviewing the literature on earlier animal models of OSCC invading the mandible, it becomes clear that the modelling techniques used in this animal model were not particularly discussed. To explore the modelling approach further and summarise the modelling experience, the present authors investigated this model through repeated multi-sample experiments in this study.

The present study established the animal model of OSCC invading the mandible through comprehensive verification of anatomical specimens, histology and imaging. Through the processing of anatomical specimens, compared with the mandible on the normal side, the texture of the posterior border of the mandible on the hormonal side became brittle, and the lower border of the mandible could be defective or locally tough, and its bone surroundings were wrapped by tumour tissues to reach the state of no resistance to needling. Through HE staining for histological processing, it was discovered that the bone's surroundings, whether sagittal or horizontal, had been infiltrated by squamous carcinoma cells and had locally displayed infiltrative destruction. MicroCT 3D scans clearly demonstrated that the mandible on the hormonal side showed erosive resorption, which further supported the success of the model.

Some researchers have utilised carcinogenic drugs to apply carcinogenicity to animals' tongues or buccal parts,[16] and there is also the approach involving drinking water carcinogenicity,[17] according to previous experience with the construction of animal models of oral cancer. Although these methods can better simulate the process of tumour growth in the organism, it is questionable whether the tumour tissues they obtain can be the same or similar to the squamous carcinoma cells of human origin after primary culture. Additionally, the operation will be rather difficult and the experimental period of these autologous transplanted tumours, which are subsequently cultivated in primary culture to produce tumours, is significantly longer.

It is well known that the construction of animal models is a relatively long and difficult process, especially the animal model of OSCC invading the mandible; there are problems regarding inexperience in the method of model construction. During the pre-test, the present authors tried to inject the tumour cell suspension into the occlusal muscle, but found that the tumour would grow to the buccal skin in an "exophytic" manner, and its size and shape of the tumour would be different. Secondly, considering that the intraoral injection of the tumour would affect the nude mice's ability to eat and breathe, the present authors finally chose the injection method mentioned above. Regarding the periosteum as a "natural barrier", they also considered whether it would hinder OSCC from invading the mandible, so designed the intervention periosteum group and the non-intervention periosteum group, and found that squamous carcinomas would damage the mandible regardless of the periosteum treatment; only the time and infiltration depth would be different. However, considering the intervention of the periosteum as an artificial factor, the subsequent experiments did not treat the periosteum.

Based on the experimental process and experience, the present authors concluded that several factors can affect the success of modelling. First, the cells themselves, including cell lineage, cell concentration, cell activity and the survival cycle of various oral squamous carcinoma cells, are significantly different. Second, the feeding environment will also have an impact on the survival cycle of nude mice. Under the SPF environment, the survival cycle of nude mice with tumour-bearing cells (CAL27 cells, injected with 1×10^6 cells/0.1 ml) is generally 1 to 2 months. In contrast, if the nude mice are in the general environment, or are constantly transferred to undergo other operations during this period, this influences the environment, which may lead to the shortening of the survival cycle. Third, for the nude mice tumour model, controlling the age of the mice is the most basic requirement. Thus, it is crucial to choose mice of an appropriate age. In this experiment, nude mice aged 4 to 6 weeks and weighing 20 ± 3 g were used, but their weight fluctuation could not be too great. Fourth, the degree of destruction of the mandible in the mandibular invasion model has a certain relationship with the survival cycle of the tumour-bearing nude mice; in other words, if the experimenter imposes certain changes in the treatment conditions or the operation, which indirectly lead to the prolongation of the survival cycle of the tumour, the degree of destruction of the mandible may also increase accordingly.

Through repeated experiments using numerous samples of various oral squamous carcinoma cells, the present findings demonstrate that, for this model, the method used in the study is straightforward, the experimental period is relatively short and the results satisfy the purpose of the experiment. Although this model is not optimal, it is the most suitable model at present. However, just as one key cannot open all doors, it is important that researchers select the best and most suitable model for their research according to their own experimental purpose, and obtain the results they want in order to cooperate to carry out the related research.

Conclusion

The animal model constructed in the present study not only mimicked the growth pattern of OSCC invading the mandible to a certain extent, but also provided a basis for conducting related research, and at the same time laid the foundation for other scholars to carry out research into the mechanism of OSCC invading the mandible, even though the present study has some shortcomings, such as the fact that the nude mice themselves have a defective immune system, which limits the development of immune-related research.

Acknowledgements

The authors thank all the study participants who contributed to this study.

Conflicts of interest

The authors declare no conflicts of interest related to this study.

Author contribution

Dr Xiang Long ZHENG performed the experiments, analysed the data and drafted the manuscript; Drs Ya Qi CHEN and Cheng Hui LU contributed to the analysis and interpretation of the data; Drs Wen LL, Kang Wei ZHOU and Li Song LIN designed the study, analysed the data and critically revised the manuscript.

(Received Sep 09, 2023, accepted Mar 12, 2024)

References

1. Botticelli A, Mezi S, Pomati G, et al. The 5-Ws of immunotherapy in head and neck cancer. Crit Rev Oncol Hematol 2020;153:103041.
2. Miao L, Lv X, Huang C, Li P, Sun Y, Jiang H. Long-term oncological outcomes after oral cancer surgery using propofol-based total intravenous anesthesia versus sevoflurane-based inhalation anesthesia: A retrospective cohort study. PLoS One 2022;17:e0268473.
3. Silva LC, Faustino ISP, Ramos JC, et al. The importance of early treatment of oral squamous cell carcinoma: Case report. Oral Oncol 2023;144:106442.
4. Fan H, Tian H, Cheng X, et al. Aberrant Kank1 expression regulates YAP to promote apoptosis and inhibit proliferation in OSCC. J Cell Physiol 2020;235:1850–1865.
5. Fukumoto C, Uchida D, Kawamata H. Diversity of the Origin of Cancer Stem Cells in Oral Squamous Cell Carcinoma and Its Clinical Implications. Cancers (Basel) 2022;14:3588.
6. Hinni ML, Ferlito A, Brandwein-Gensler MS, et al. Surgical margins in head and neck cancer: a contemporary review. Head Neck 2013;35:1362–1370.
7. Goldschmidt S. Surgical Margins for Ameloblastoma in Dogs: A Review With an Emphasis on the Future. Frontiers in Veterinary Science 2022;9:830258.
8. Moratin J, Horn D, Metzger K, et al. Squamous cell carcinoma of the mandible – Patterns of metastasis and disease recurrence in dependence of localization and therapy. J Craniomaxillofac Surg 2020;48:1158–1163.
9. Michalek J, Brychtova S, Pink R, Dvorak Z. Prognostic and predictive markers for perineural and bone invasion of oral squamous cell carcinoma. Biomed Pap Med Fac Univ Palacky Olomouc Czech Repub 2019;163:302–308.
10. Supsavhad W, Dirksen WP, Martin CK, Rosol TJ. Animal models of head and neck squamous cell carcinoma. Vet J 2016;210:7–16.
11. van der Worp HB, Howells DW, Sena ES, et al. Can Animal Models of Disease Reliably Inform Human Studies? PLoS Med 2010;7:e1000245.
12. Nomura T, Shibahara T, Katakura A, Matsubara S, Takano N. Establishment of a murine model of bone invasion by oral squamous cell carcinoma. Oral Oncol 2007;43:257–262.
13. Lee JK, Lim SC, Kim HD, et al. KITENIN represents a more aggressive phenotype in a murine model of oral cavity squamous carcinoma. Otolaryngol Head Neck Surg 2010;142:747–752.e741-742.
14. Furuta H, Osawa K, Shin M, et al. Selective inhibition of NF-κB suppresses bone invasion by oral squamous cell carcinoma in vivo. Int J Cancer 2012;131:E625–E635.
15. Salley JJ. Experimental carcinogenesis in the cheek pouch of the Syrian hamster. J Dent Res 1954;33:253–262.
16. Tanaka T, Kawabata K, Kakumoto M, et al. Chemoprevention of 4-nitroquinoline 1-oxide-induced oral carcinogenesis by citrus auraptene in rats. Carcinogenesis 1998;19:425–431.
17. Yu L, Liu XQ, Chen YH, Chen X, Nie MH. Study on expression of LIM domain only protein 1 in SD rat oral buccal mucosa carcinogenesis induced by 4-nitro-quinoline N-oxide [in Chinese]. Hua Xi Kou Qiang Yi Xue Za Zhi 2020;38:133–138.